Bull Earthquake Eng
DOI 10.1007/s10518-010-9178-6

ORIGINAL RESEARCH PAPER

On the use of JMA intensity in earthquake early warning systems

Vladimir Sokolov · Takashi Furumura · Friedemann Wenzel

Received: 10 July 2009 / Accepted: 23 February 2010

Abstract The estimation of strength of shaking at a site from the initial P-wave portion of ground motion is the key problems for shortening the alert time of the earthquake Early Warning (EEW). The most of the techniques proposed for the purpose utilize (a) ground motion models based on the estimated magnitude and hypocentral distance, or (b) the interim proxies, such as initial vertical displacement P_d. We suggest the instrumental Japan Meteorological Agency (JMA) intensity (JMA_I) as a characteristic for fast estimation of damage potential in the EEW systems. We investigated the scaling relations between JMA_I measured using the whole earthquake recordings (overall intensity) and using particular time intervals of various duration (2.0–8.0 s) starting from the P-wave arrival (preliminary intensity). The dataset included 3,660 records (K-NET and the KiK-net networks) from 55 events (M_W 4.1–7.4) occurred in 1999–2008 in Japan. We showed that the time interval of 4–5 s from the P-wave arrival can be used for reliable estimations of the overall intensity with the average standard error of about 0.5 JMA units. The uncertainty in the prediction may be reduced by consideration of local site conditions or by development of the station-specific models.

Keywords Earthquake early warning · JMA seismic intensity · K-Net and KiK-net networks

V. Sokolov (✉) · F. Wenzel
Geophysical Institute, Karlsruhe Institute of Technology (KIT), Hertzstr. 16, 76187 Karlsruhe, Germany
e-mail: Vladimir.Sokolov@kit.edu

F. Wenzel
e-mail: Friedemann.Wenzel@kit.edu

T. Furumura
Earthquake Research Institute, University of Tokyo, 1-1-1, Bunkyo-ku, Tokyo, Japan
e-mail: Furumura@eri.u-tokyo.ac.jp

Published online: 19 March 2010

1 Introduction

Real-time seismology deals with collection and quick analysis of the data after a seismic event. The information is used for the warning purposes or post-earthquake emergency response. The "Earthquake Early Warning" (EEW) systems utilize the time difference between the moments when (1) the relatively small-amplitude and rapidly propagating primary (P) waves and (2) the damaging large-amplitude and slowly propagating secondary (S) waves would reach the site. The time difference, in some cases, may reach several tens of seconds. The recent advances in seismology, sensor, computer and telemetry technologies allow constructing the effective "early-warning" systems (e.g. Aoi et al. 2008; Hoshiba et al. 2008).

In principle, there are two types of the earthquake early-warning issues (e.g. Kanamori 2005; Wu and Kanamori 2005; Allen et al. 2009), namely: (1) determination of parameters of the occurred earthquake (magnitude and location), (2) estimation of damage potential (macroseismic intensity, peak amplitudes, etc.) of the strongest portion of seismic shaking at a site (so-called on-site warning) with no necessary attempt to locate the event and evaluate the magnitude. On one hand, the magnitude and location of the earthquake, which were determined during the first task, may be used to resolve the second task by calculation of ground motion parameters at a given site with the aid of regional strong-motion prediction equations (e.g. Allen 2004, 2007; Hoshiba et al. 2008). On other hand, the relations between the parameters of the initial portion of P-wave and the characteristics of subsequent strong shaking may be used for estimation of damage potential at given site (Wu and Kanamori 2005; Nakamura and Saita 2007; Wu et al. 2007; Kanda et al. 2008; Yamamoto et al. 2008). This approach may be very fast and could provide useful early warning even at very short epicentral distances.

Seismic intensity is still an essential parameter of earthquake ground motion allowing a simple and understandable description of earthquake damage. For example, the intensity level defined by the Japanese Meteorological Agency (JMA) has 10 ranks (0–4, 5 lower/upper, 6 lower/upper, and 7). The EEW should be issued to the general publics when the seismic signals are detected at two or more stations and the anticipated maximum seismic intensity is equal to or exceeds "5lower" (JMA scale) (Hoshiba et al. 2008; Doi et al. 2008; Kamigaichi et al. 2009). Seismic intensity "5Lower" on the JMA scale approximately corresponds to VII–VIII on the modified Mercalli scale. Actually, the intensity level should be predicted for large areas. For some limited users (e.g. railway companies, elevator companies, and manufacturing industries), the EEW describes information on the hypocentral parameters (latitude, longitude, focal depth, origin time, and magnitude), anticipated maximum seismic intensity, and earliest arrival time of *S* waves for districts where seismic intensity is predicted to be equal to 4 or greater on the JMA scale (Hoshiba et al. 2008). Seismic intensity 4 on the JMA scale approximately corresponds to VI or VII on the modified Mercalli scale. Warnings are updated when the seismic intensity is anticipated to be equal to "5Lower" or greater at districts (Japanese Islands are divided into about 200 divisions) where the estimated intensity was less than JMA 4 in the first warnings.

Thus, there is a necessity of quick estimation of the maximum expected intensity and the updated estimations. Application of the ground motion models, which are based on estimated magnitude and distance and which include site amplification coefficients (e.g. Hoshiba et al. 2008; Ueda et al. 2008), or consideration of the interim proxies such as initial vertical displacement P_d (Wu and Kanamori 2005; Wu et al. 2007) or Damage Index (Nakamura and Saita 2007), may introduce additional uncertainty. We suggest the instrumental JMA (JMA_I) intensity as a proper characteristic for fast estimation of damage potential in EEW systems. The JMA_I intensity is calculated using three-components accelerogram after applying a proper band-pass filter to enhance characteristic frequencies of around 0.5–2 Hz that characterize strong motion damage of wooden-frame houses and man-felt shaking (http://www.hp1039.jishin.go.jp/eqchreng/at2-4.htm). We rely on such JMA_I for robust and reliable estimation of strong motion disasters than using conventional intensity estimate such as adopted in MM of MSK scales. If necessary, the JMA_I estimations may be recalculated to values of MM or MSK scales using proper equations derived empirically based on regression analysis (Shabestari and Yamazaki 2001; Sokolov and Furumura 2008).

The possibility of the use of instrumental JMA intensity in the EEW systems has been recently analyzed by Yamamoto et al. (2008). The authors compared intensities estimations based on a 6-s window after the P-wave arrival (P-wave intensity) and on S-wave window (S-wave intensity). A new parameter called "intensity magnitude" M_I was introduced. The parameter is based on the intensity estimations from the P-wave data and additional information about source-to-site distance and path attenuation parameters. The expected S-wave intensity is evaluated from the computed M_I value.

In this study we made an attempt to develop the on-site warning technique based on direct estimation of JMA intensity. We investigated the scaling relationships between the JMA instrumental intensity measured using (a) the whole earthquake recordings (hereafter we denote JMA_O, overall intensity) and (b) the particular time intervals of various durations (2.0, 3.0,…,8.0 s) starting from the P-wave arrival (hereafter we denote JMA_P, preliminary intensity). We also consider, as additional parameters in the scaling relations, the earthquake magnitude and hypocentral distance, and so-called characteristics period τ_C (Kanamori 2005; Wu and Kanamori 2005) determined from the early portion of seismic record. The performance of the relationships in respect of its utilization in the EEW issues has been studied.

2 The data

The dataset includes 3,660 records from 55 events with magnitude range M_W 4.1–7.4 occurred in 1999–2008. The earthquakes were recorded by the K-NET and the KiK-net nation-wide strong motion networks over 1800 strong motion instruments, which have been deployed across Japan by the National Research Institute for Earth Science and Disaster Prevention (NIED) since 1996. The K-NET strong motion network is distributed uniformly along the Japanese Islands at intervals of about 25 km (Kinoshita 1998). Three-component accelerometers are installed at free field of populated area such as at school yard in elementary and junior high schools and around the city office. The KiK-net is also distributed across Japan at uniform interval of about 25 km, some of them are placed in the city but most of them are placed at a hill side of quiet place in suburbs, since it is a complex facility with the Hi-net high-gain seismic network (Aoi et al. 2000). The KiK-net has three-component accelerometers installed in borehole of about 100–3,000 m deep, depending on the depth of hard rock (Vs > 3,000 m/s), as well as at free-field. These acceleration records have been obtained from sites http://www.kyoshin.bosai.go.jp/index_en.html. Figure 1 shows stations in the K-NET and KiK-net networks across Japan and the epicenters of earthquakes used in the present study. Note that in this study we used only free-field records.

We used moment magnitude in our analysis rather than the JMA estimates (M_J). Therefore, for the cases when the magnitude data contain information about another type of magnitude, the correspondent estimations were obtained from Harvard seismic catalogue http://www.seismology.harvard.edu/.

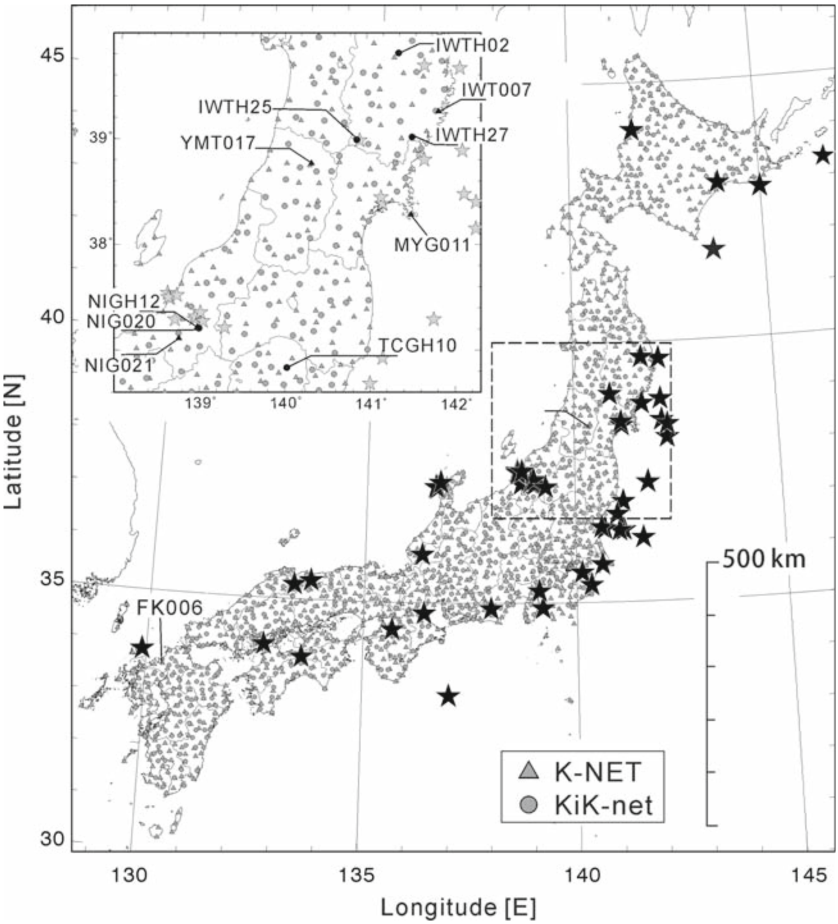

Fig. 1 Stations in the K-NET and KiK-net networks across Japan and the epicenters of earthquakes used in the present study. Specific K-NET and KiK-net stations are marked

3 Analysis

In our study we calculated the JMA instrumental intensity for the whole record (JMA_O, overall intensity) and for the particular time intervals of various durations (2.0, 3.0,…, 8.0 s) starting from the P-wave arrival (JMA_P, preliminary intensity). The visual inspection was used for selection of the moment of P-wave arrival. Formally, the JMA instrumental intensity is calculated using whole waveform data of three-component accelerograms including P and S waves. However, the instrumental intensity can also be calculated successively at every one second and even on real time (Aoi et al. 2008; Kunugi et al. 2008). In our study we used the same procedure for calculation of JMA_O and JMA_P intensity.

The selected time intervals, depending on site-to-source distance, may contain also the S-wave phase. However, for consistency we call the intervals as the P-wave window. Figure 2 shows examples of records and time dependency of the preliminary intensity estimations. Distribution of the JMA_O–JMA_P pairs for various P-wave windows is shown in Fig. 3.

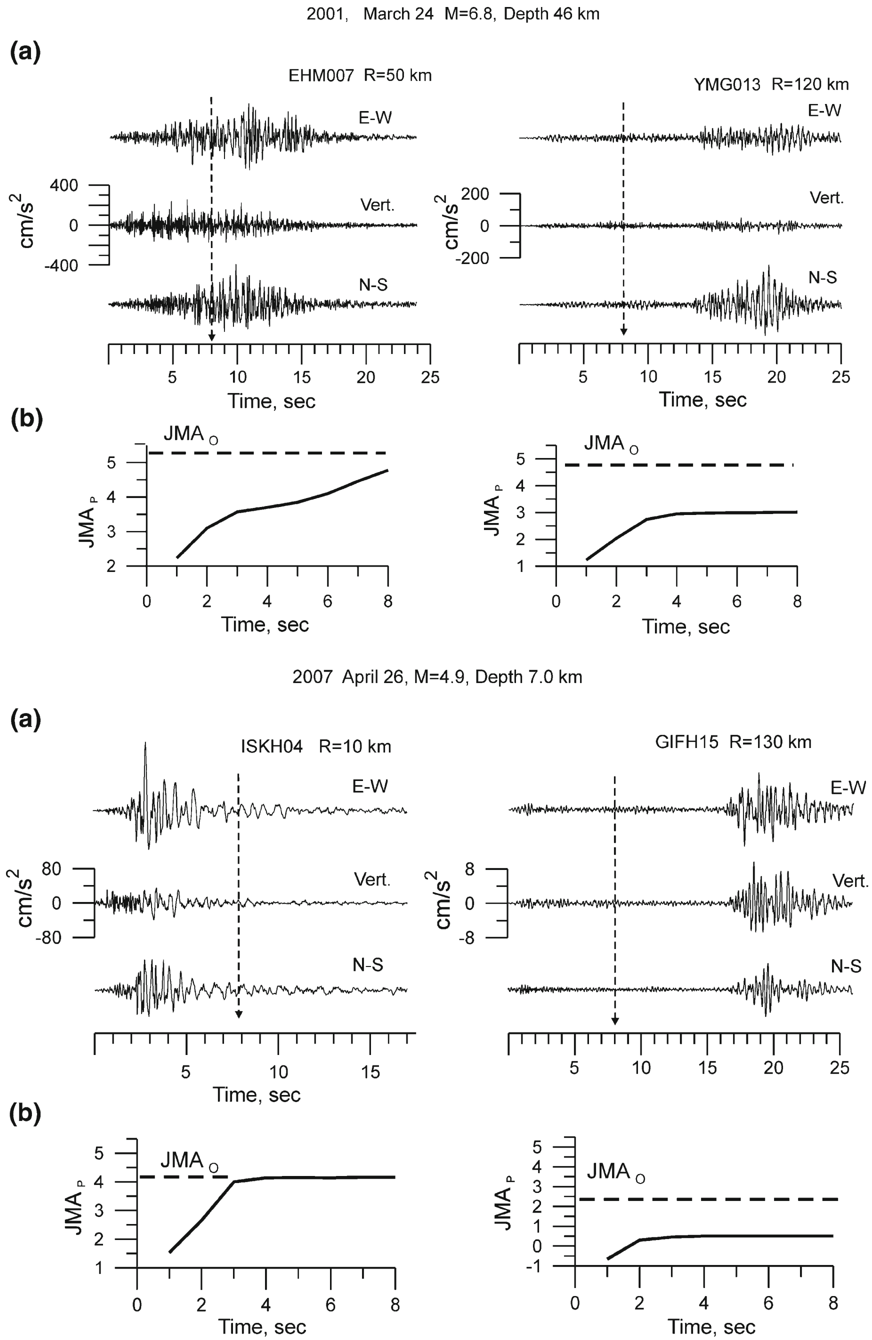

Fig. 2 Estimation of JMA intensity for earthquake early warning purpose. **a** Ground motion records (acceleration, cm/s^2) obtained at two stations located at different hypocentral distances R from the same earthquake. *Dashed lines mark* the first 8 s from the P-wave arrival. **b** Time-dependent nature of the JMA_P intensity estimated from the initial portions of P-wave using various time intervals. *Dashed line* show the values of instrumental intensity calculated for the whole earthquake record (JMA_O)

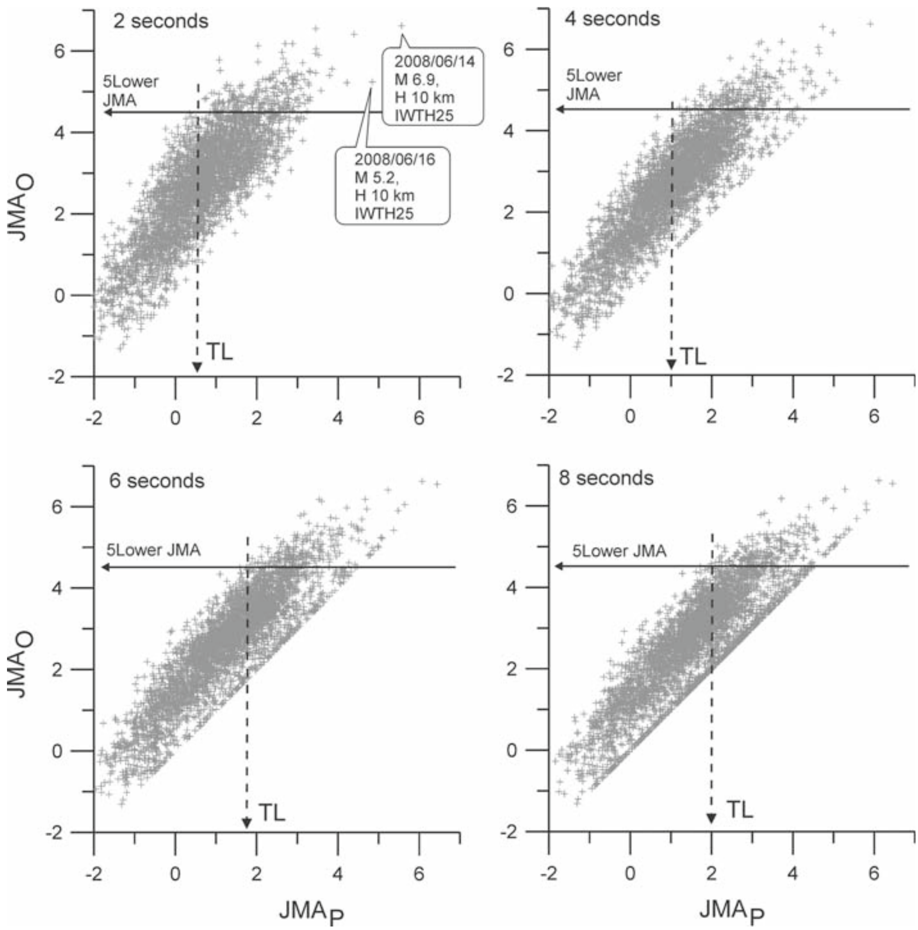

Fig. 3 Distribution of the JMA instrumental intensity calculated for the entire earthquake records (JMA_O) versus the intensity estimated for the initial portions of ground motion (JMA_P) using various time intervals (2, 4, 6, and 8 s) after the P-wave arrival. *Arrows mark* the levels of JMA intensity for the EEW issues (*solid lines*) and correspondent threshold levels TL of JMA_P (*dashed lines*)

The level "5Lower" of JMA_O that should be considered in the EEW issues correspond to the instrumental intensity of at 4.5 JMA_I (http://www.hp1039.jishin.go.jp/eqchreng/at2-4.htm). As can be seen from Fig. 3, the values of preliminary intensity JMA_P are generally less than JMA_I 4.5 for the P-wave windows with length less than 3–4 s, except a few particular cases for the events of very short hypocentral distances. At the same time, the preliminary intensity may become almost equal to the overall intensity, after 3–4 s from the P-wave arrival (Fig. 3). It means that the major shaking has already occurred during this time interval (Fig. 2, event of April 26, 2007, station ISKH04).

Based on distribution of observed JMA_O–JMA_P pairs, it is possible to choose a threshold level (TL) of the preliminary intensity, which can be considered when predicting the overall intensities and checking for the possible EEW issue, i.e. "5Lower" JMA. For the 2-s time interval, for example, the threshold level is about 0.5 JMA_{P2} for 4.5 JMA_I or "5Lower" JMA. Here index "P2" denotes the preliminary intensity estimated from 2-s P-wave window.

In other words, if the observed JMA_{P2} value at a station is more than 0.5 JMA_I, there is a non-zero probability that the value of overall intensity will be more that 4.5 JMA_I. Consequently, if the observed JMA_{P2} value is less than 0.5 JMA_I, there is no necessity for evaluation of the overall intensity for the EEW issue. As expected, the threshold levels change with the increase of length of the P-wave window and, for the 8-s P-wave window, they reach the value of 2.0 JMA_{P8}.

The question what we would like to consider in this study is the following—how precisely we can predict the overall JMA intensity (JMA_O) based on estimations of the preliminary intensity (JMA_P) calculated from the first few seconds of ground motion recording after the P-wave arrival?

Let us analyze the relationship between the overall intensity and the preliminary intensity and consider the case when no information about parameters of the recorded earthquake (magnitude, distance, and depth) is available—so-called "blind" estimation. The parameters of a function that relate two variables usually are estimated using the least squares technique. In ordinary least squares (OLS), the independent (predictor) variables (X) is assumed to be measured without error and all of the errors are in the dependent (response) variables (Y). The OLS procedure, or OLS (Y|X), minimizes the sum of the squared deviation (or residual sum of squares) from the observations.

We work with the JMA instrumental intensity, which is determined using simple mathematical procedures from strong-motion records (see, for details, http://www.hp1039.jishin.go.jp/eqchreng/at2-4.htm; Shabestari and Yamazaki 2001; Sokolov and Furumura 2008). Thus, if we consider the instrumental intensity as a characteristic of a given ground motion recorded at a specific site, we can accept the requirement of a non-error predictor ($JMA_{P)}$ in the OLS analysis. The errors in the response variable (JMA_O), in this case, are caused by the factors that affect the amplitude and the frequency content of P- and S-wave in a different manner (e.g. peculiarities of source of rupture, propagation path and local site geology).

Figure 4a shows, as the examples, distribution of the JMA_O–JMA_P pairs for the 2-s and the 6-s P-wave windows. The relation between the overall intensity (JMA_O) and the preliminary intensity (JMA_P) were estimated using the following assumptions. First, when considering the time intervals that are longer than 3 s, we deleted the records, for which the difference between the overall and the preliminary intensities does not exceed 0.25 units. Thus, we excluded the cases, for which the major shaking has already occurred during the considered time window.

Second, the analyzed data are unbalanced and appear to be heteroscedastic, i.e., the variables apparently have different variances. One of the simplest ways to correct for the effect of the imbalanced data is the application of unweighted analysis of cell means. However, in this case we will lose information about the earthquake magnitude and the distance for particular observations. Another technique, which is also applied to treat heteroscedasticity, is to use the weighted least squares scheme. As a rule, weights are given as the inverse of variance, giving points with lower variance greater statistical weight. However, should we apply greater weights to large intensity points because there are only a few observations (and lower variance), or because the large intensity range is of great importance? When the weights are estimated using only a few observations, the results of an analysis can be affected in an unpredictable manner. Therefore, we assumed that each observation brings an equal contribution to the final parameter estimates.

This apparent imbalance is caused by a large difference among the sizes of the observations. Large earthquakes produce many more small and intermediate intensity records than records for large intensities. We will never obtain an equal number of observations for every

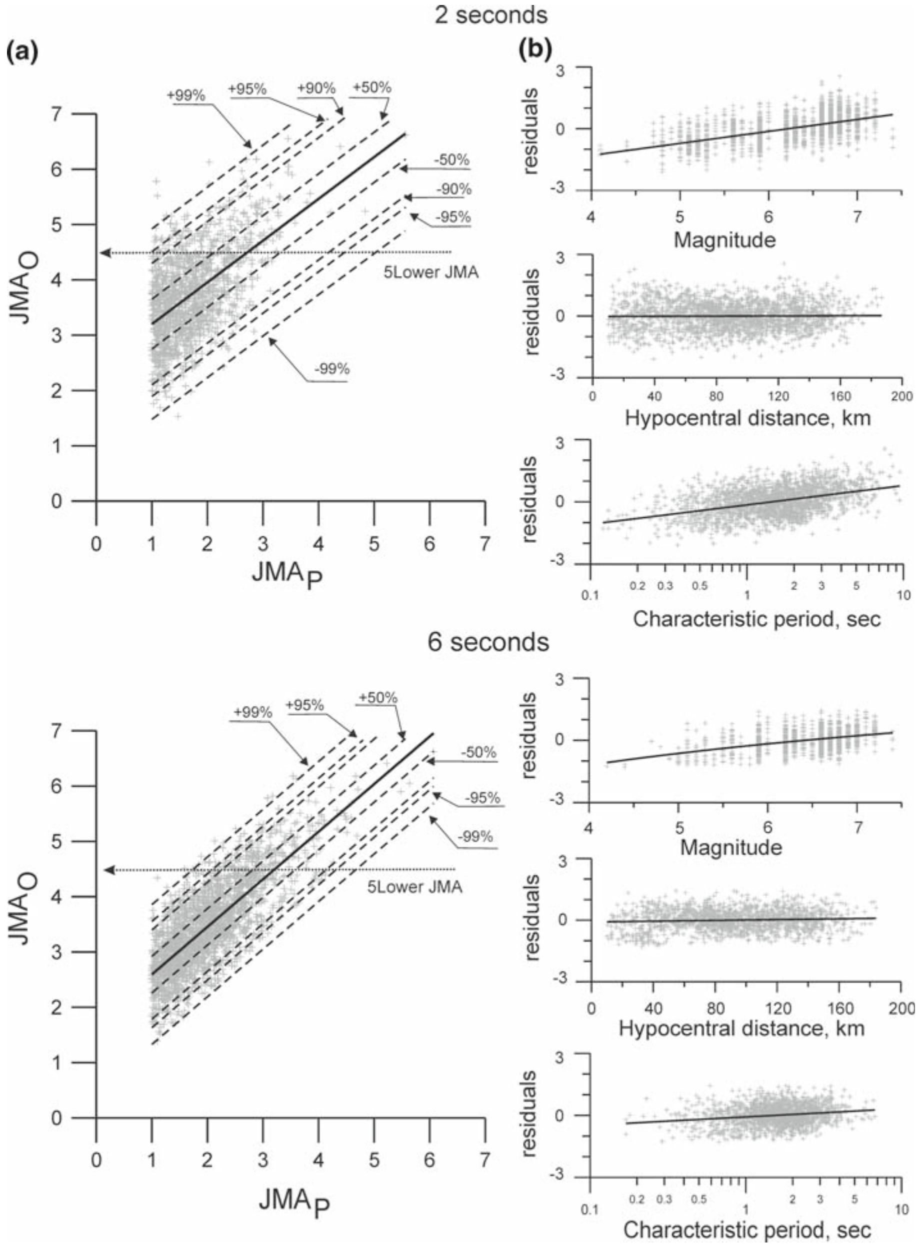

Fig. 4 Relationship between the overall intensity (JMA_O) and the preliminary intensity (JMA_P). **a** Linear OLS regression (*solid line*) and confidence limits (*dashed lines*). **b** distribution of residuals versus magnitude, epicentral distance and characteristic period. The residuals were calculated as residuals $= JMA_O - (a + bJMA_P)$

range of intensity without artificial sampling from small and intermediate intensities. There is an inherent peculiarity of such types of data.

The linear relationships $\mathrm{JMA_O} = a + b\mathrm{JMA_P}$ between the overall intensity ($\mathrm{JMA_O}$) and the preliminary intensity ($\mathrm{JMA_P}$), as well as the confidence limits, estimated for the 2 and 6-s time intervals from the P-wave arrival are shown in Fig. 4a. The linear relationships, are as follows

$$\mathrm{JMA_O} = 2.375 + 0.791\,\mathrm{JMA_{P2}} \quad [\pm 0.67] \quad 2\,\mathrm{s} \tag{1}$$

$$\mathrm{JMA_O} = 1.814 + 0.829\,\mathrm{JMA_{P2}} \quad [\pm 0.49] \quad 6\,\mathrm{s} \tag{1a}$$

where the values in square brackets denote the standard error σ of regression.

As can be seen from Fig. 4a, there is a high scatter in the $\mathrm{JMA_O}$–$\mathrm{JMA_P}$ relation for the initial stage of earthquake ground motion. The scatter exhibits clear dependence on earthquake magnitude and much lower dependence on distance (Fig. 4b). Therefore, we also checked the regressions, in which $\mathrm{JMA_O}$ depends also on magnitude M and hypocentral distance R as $\mathrm{JMA_O} = a + b\mathrm{JMA_{P2}} + cM$ and $\mathrm{JMA_O} = a + b\mathrm{JMA_{P6}} + cM + dR$. The following equations were obtained

$$\mathrm{JMA_O} = -1.213 \; + 0.706\,\mathrm{JMA_{P2}} + 0.595\; M_\mathrm{W} \quad [\pm 0.56] \quad \text{for } 2\,\mathrm{s} \tag{2}$$

$$\mathrm{JMA_O} = -0.795 \; + 0.781\mathrm{JMA_{P6}} + 0.422\; M_\mathrm{W} \quad [\pm 0.45] \quad \text{for } 6\,\mathrm{s} \tag{2a}$$

$$\mathrm{JMA_O} = -0.290 \; + 0.547\mathrm{JMA_{P2}} + 0.833\; M_\mathrm{W} - 1.15 \log_{10} R \quad [\pm 0.51] \quad \text{for } 2\,\mathrm{s} \tag{3}$$

$$\mathrm{JMA_O} = -0.425 \; + 0.708\mathrm{JMA_{P6}} + 0.507\; M_\mathrm{W} - 0.388 \log_{10} R \quad [\pm 0.45] \quad \text{for } 6\,\mathrm{s} \tag{3a}$$

The joint consideration of magnitude and preliminary intensity $\mathrm{JMA_P}$ allows obtaining a sufficient increase of the accuracy of overall intensity estimations, as compared with the "blind" estimation. Consideration of hypocentral distance does not reduce significantly standard error of the relationships.

However, could we obtain a reasonably good estimations of the overall intensity without information on earthquake magnitude? There is a parameter, which can be used as a proxy of magnitude and which can be calculated from vertical component of the record based on the same time interval from the P-wave arrival, namely: the characteristic period τ_C (Kanamori 2005; Wu and Kanamori 2005). Sokolov et al. (2009) analyzed performance of scaling relation between moment magnitude and characteristic period using the same database that has been used in this work. The regression equation, in which $\mathrm{JMA_O}$ depends also on the characteristic period are the following

$$\mathrm{JMA_O} = 2.224 \; + 0.793\mathrm{JMA_{P2}} + 0.932 \; \log_{10}(\tau_C) \quad [\pm 0.60] \quad \text{for } 2\,\mathrm{s} \tag{4}$$

$$\mathrm{JMA_O} = 1.738 \; + 0.830\mathrm{JMA_{P6}} + 0.404 \; \log_{10}(\tau_C) \quad [\pm 0.48] \quad \text{for } 6\,\mathrm{s} \tag{4a}$$

As can be seen, consideration of the characteristic period also allows increasing, even if slightly, the accuracy of the overall intensity estimation as compared with the use of the $\mathrm{JMA_P}$ parameter only. Note that the τ_C values were calculated from the same time windows as used for calculation of the $\mathrm{JMA_P}$ values.

Distribution of residuals, i. e. difference between the actual values of the overall intensity and the values predicted using corresponding equations of multiple regression, versus the

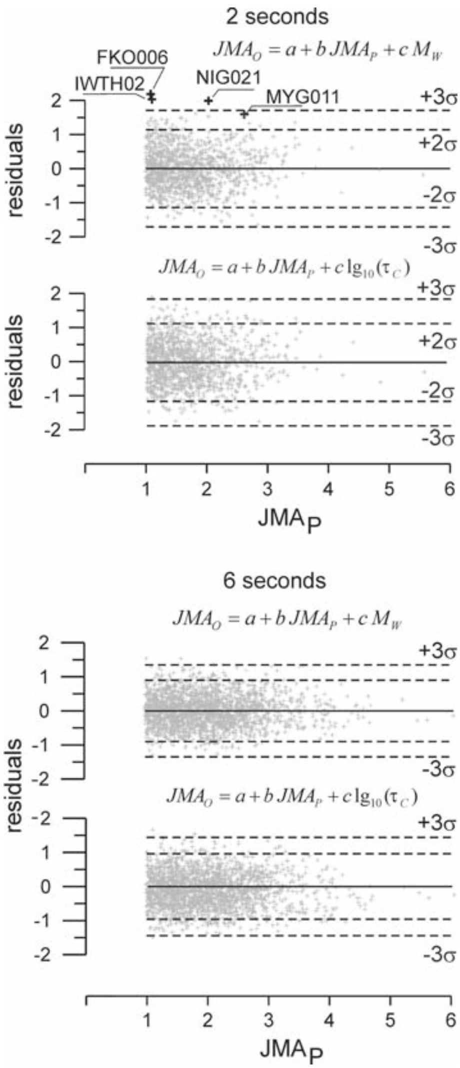

Fig. 5 Distribution of residuals, which were calculated as difference between the actual values of the overall intensity (JMA_O) and the values predicted using linear relationships that consider earthquake magnitude M_W or characteristic period τ_C. The confidence levels evaluated using the standard errors σ of regression are shown by *dashed lines*. Particular cases of large residuals and failed predictions of the "5 lower JMA" level are marked by the stations names (see Table 1)

preliminary intensity is shown in Fig. 5. There are a few cases when the residual can exceed a value of $+3\sigma$(standard error of regression) for the 2-s interval. The underestimation of the overall intensity is particularly important when the scaling relation fails to predict the "5Lower JMA" level used in the EEW issues. Such extreme cases of failed prediction (small JMA_{P2}–large JMA_O) are listed in Table 1. At the same time, the cases of overestimation of the overall intensity are also of interest, especially when the scaling relation resulted in estimated values that are larger that JMA_O 4.5 ("5Lower" JMA, false alarm). Such cases are also listed in Table 1. Location of the considered stations is shown in Fig. 1 and the correspondent records are shown in Fig. 6.

The calculated value of the instrumental JMA intensity depends on amplitude of the vectoral composition of the three components of band-pass filtered ground acceleration record (http://www.hp1039.jishin.go.jp/eqchreng/at2-4.htm, see also Shabestari and

Table 1 Results of evaluation of overall intensity using the predictive scaling relations based on obtained values of preliminary intensity

Station	Overall JMA	Time interval 2 s			Time interval 6 s		
		JMA_{P2}	Predicted JMA		JMA_{P6}	Predicted JMA	
			Eq. 6[a]	Eq. 8[b]		Eq. 6a[a]	Eq. 8a[b]
Underestimation of overall intensity							
FKO006	5.5	1.1	3.5 (2)	4.0 (1.5)	3.5	4.7 (0.8)	4.8 (0.7)
IWTH02	5.8	1.1	3.6 (2.2)	3.9 (1.9)	3.1	4.4 (1.4)	4.5 (1.3)
NIG021	6.1	2.0	4.1 (2.0)	4.3 (1.9)	3.6	4.8 (1.3)	4.9 (1.2)
Overestimation of overall intensity							
TCGH10	3.0	2.8	4.7 (1.7)	4.9 (1.9)	–	–	–
YMT017	3.5	2.7	4.9 (1.4)	4.7 (1.2)	2.8	4.3 (0.8)	4.1 (0.6)

The records are shown in Fig. 6 together with information about the earthquakes
[a] predictions based on magnitude M_W
[b] predictions based on characteristic period τ_C

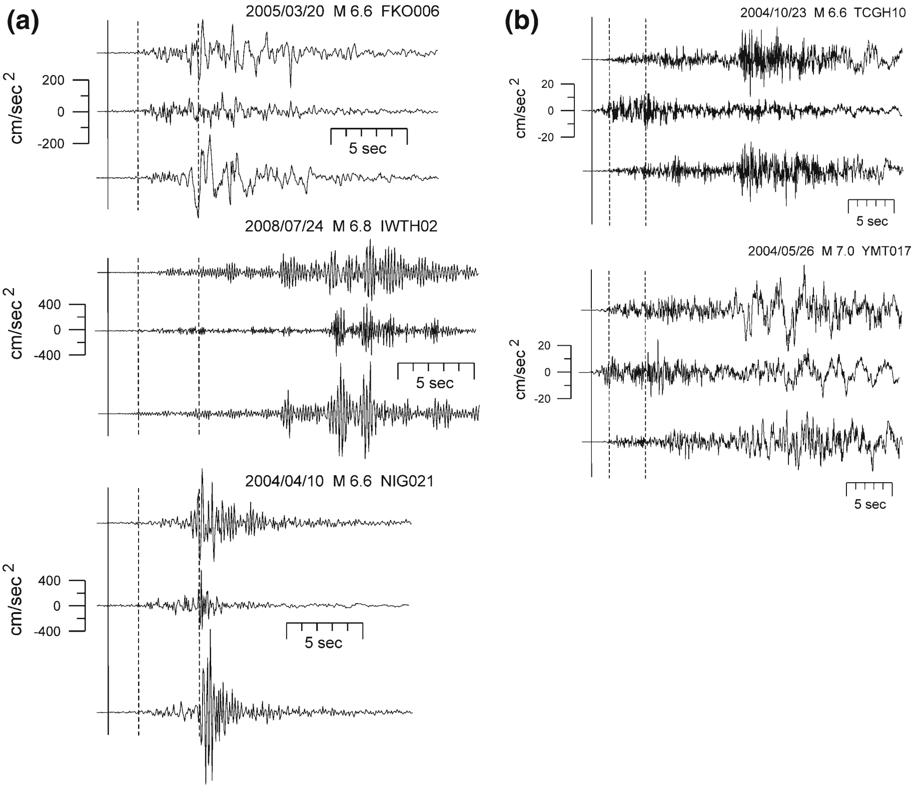

Fig. 6 Acceleration records for the cases listed in Table 1. *Dashed vertical lines mark* the time intervals (2 and 6 s) from the P-wave arrival (*solid vertical lines*) used for calculation of preliminary intensity. **a** Small JMA_{P2}–large $JMA_{O,}$ underestimation of the overall intensity; **b** large JMA_{P2}–small $JMA_{O,}$ overestimation of the overall intensity

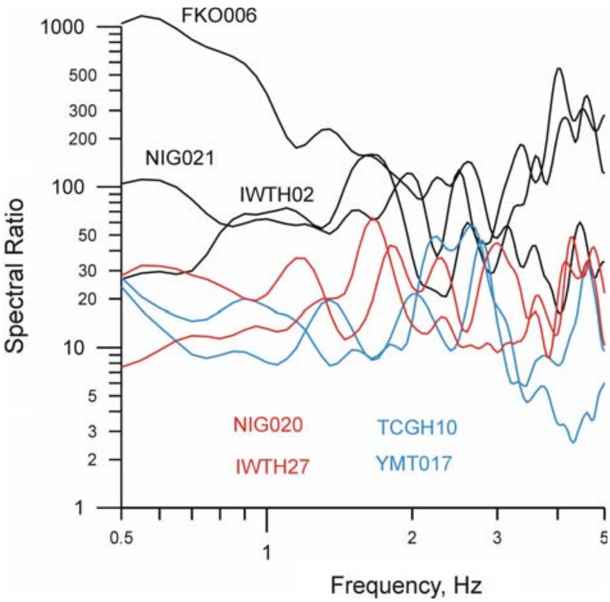

Fig. 7 Ratios between the vectorial composition of Fourier amplitude spectra of the whole records and the 2-s P-wave window (see text, Eq. 5)

Yamazaki 2001). The band-pass filter is characterized by maximum amplitude at frequencies of 0.5 Hz. Thus, the procedure of JMA calculation is sensitive to peculiarities of spectra around this frequency range (Sokolov and Furumura 2008). We selected the most extreme cases of failed prediction (underestimation and overestimation) based on the 2-s P-wave window, as well as a few records of almost zero residuals between the actual values of overall intensity and the estimations (successful prediction). Figure 7 shows ratios (VCR) between vectorial compositions of Fourier amplitude spectra of the whole records and the 2-s P-wave window used for estimation of preliminary intensity $\mathrm{JMA_{P2}}$ for the considered cases. The ratios were calculated as

$$\mathrm{VCR}(f) = \mathrm{VR_O}(f)/\mathrm{VC_{P2}}(f), \quad \mathrm{VC}(f) = \sqrt{\mathrm{FAS}^2_{\mathrm{NS}}(f) + \mathrm{FAS}^2_{\mathrm{EW}}(f) + \mathrm{FAS}^2_{\mathrm{UP}}(f)} \quad (5)$$

where $\mathrm{FAS_{NN}}(f)$ is the amplitude of Fourier spectrum of particular component NN. The cases of extreme underestimation (small $\mathrm{JMA_{P2}}$–large $\mathrm{JMA_O}$, stations FKO002, NIG021 and IWTH02) are characterized by the larger VCR amplitudes for frequencies below 2–3 Hz than the cases of successful prediction (stations NIG020 and IWTH27). The amplitudes of the initial portion of P-wave are very small in all these cases (Fig. 6) and this phenomenon causes the large $\mathrm{JMA_O}$–$\mathrm{JMA_{P2}}$ ratios. Correspondingly, the cases of overestimation (stations TCGH10 and YMT017) show relatively high amplitudes of the initial portion of P-wave that resulted in the lower VCR amplitudes than that for the cases of successful prediction for frequencies below 2.0 Hz.

Some of the considered stations accumulated several earthquake records and we checked distribution of the residuals versus magnitude, hypocentral distance and overall intensity (Fig. 8). As can be seen, the cases of underestimation of the overall intensity (large positive values of the residuals) were observed at station NIG021 for small distances, large magnitudes and large JMA values; while station IWTH02 exhibits large positive residuals only for

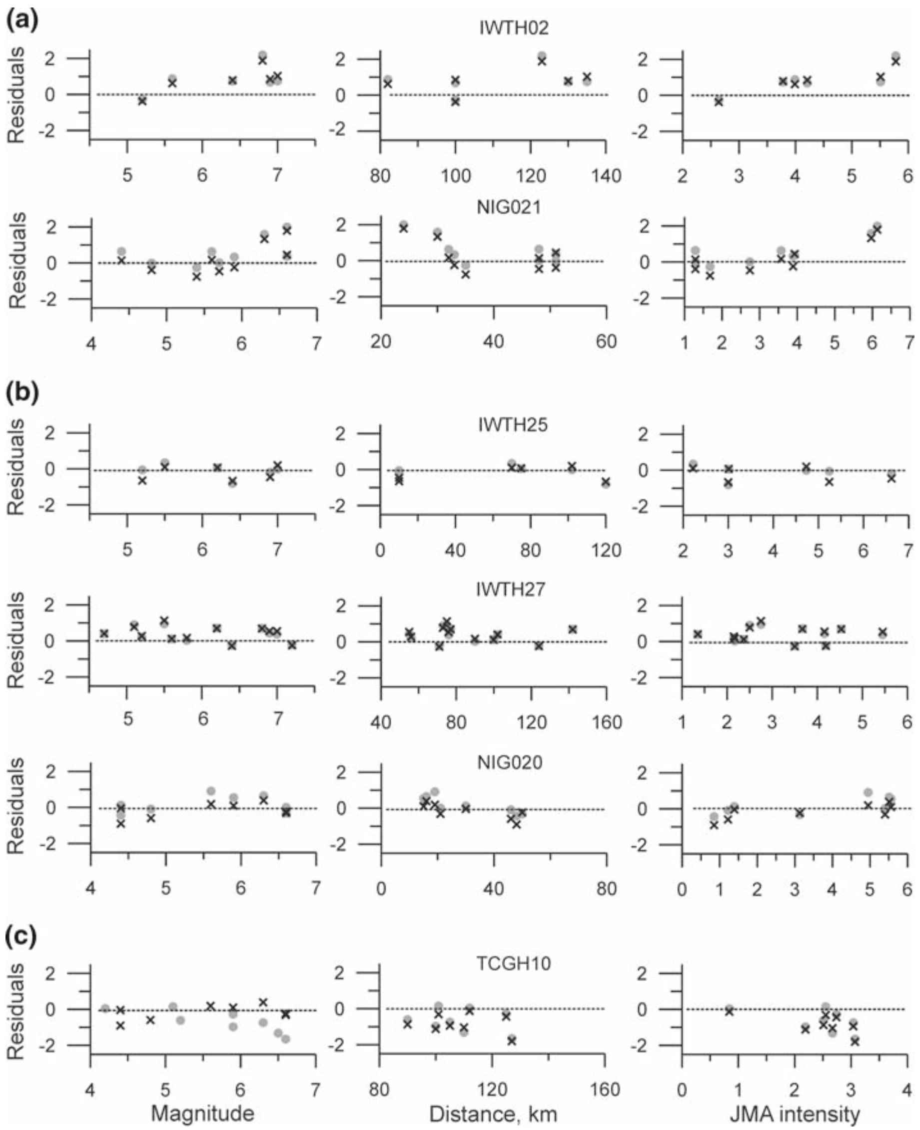

Fig. 8 Distribution of residuals, or difference between the actual values of the overall intensity and the values predicted using empirical regressions, versus magnitude, distance and overall intensity for selected stations. Circles—values predicted using magnitude (Eq. 2); crosses—values predicted using characteristic period (Eq. 4). **a** stations revealed underestimation of overall intensity; **b** stations revealed successful prediction; **c** station revealed overestimation of overall intensity

one large and distant earthquake (see Table 2 for characteristics of the earthquakes). For the cases of successful prediction (stations IWTH25, IWTH27, and NIG020), the residuals are small and distribution of the residuals does not show dependence on magnitude, distance, or JMA intensity. The data from station TCGH10 reveal the negative residuals (overestimation of overall intensity) for almost all recorded earthquake; and one case (M 6.6, R 120 km, 23 October 2004) might result in a false alarm.

Table 2 Characteristics of the recordings used for analysis of the cases of failed and successful estimations of the overall intensity based on the 2-s P-wave window (see also Figs. 7 and 8)

Station	Date	JMA	Magnitude	Depth (km)	Distance (km)
Underestimation (see also Fig. 8a)					
FKO002	20 March 2005	5.5	6.6	7	27
IWTH02	24 July 2008	5.8	6.8	120	140
NIG021	23 October 2004	6.1	6.6	13	24
NIG021	23 October 2004	6.0	6.3	14	30
Successful prediction (see also Fig. 8b)					
IWTH27	26 May 2003	5.5	7.0	70	140
IWTH25	14 June 2008	6.6	6.9	10	11
NIG020	23 October 2004	5.4	6.6	13	26
Overestimation (see also Fig. 8c)					
TCGH10	23 October 2004	3.0	6.6	13	120
YMT017	26 May 2003	3.5	7.0	70	135

Table 3 Description of soil columns for stations listed in Table 1

Station	Description of local geology
FKO006	Sandy and gravelly soil with small S-wave velocity ($V_S = 200$–$400\,$m/s) and relatively high P-wave velocity ($V_P = 1{,}500$–$2{,}000\,$m/s).
IWTH02	A thin (5 m), very soft ($V_S = 150\,$m/s and $V_P = 300\,$m/s) humus and soft clayey soil ($V_S = 460$–$780\,$m/s, $V_P = 1{,}800$–$2{,}300\,$m/s) of about 20 m thick covers hard sedimentary rock ($V_S = 1{,}300$–$2{,}300\,$m/s, $V_P = 3{,}400$–$4{,}500\,$m/s) with very large velocity contrast between layers.
NIG021	A thin (5–7 m) layer of gravelly soil ($V_S < 400\,$m/s, $V_P < 1{,}500\,$m/s) over soft rock ($V_S > 500\,$m/s, $V_P < 2, 100\,$m/s).
TCGH10	Gravel ($V_S > 500\,$m/s, $V_P > 1{,}600\,$m/s) of about 60 m thick covers volcanic rock ($V_S = 800$–$900\,$m/s, $V_P = 2{,}200\,$m/s).
YMT017	No information

It is reasonable to suggest that the cases of underestimation and overestimation of the overall intensity reflect the phenomena, which influence on frequency content of the P-wave and the S-wave portions in different manner (e.g. directivity effect especially for small epicentral distances, high-frequency radiation from a deep, high stress-drop sources, effects of propagation path, local site amplification, non-linear effects in soil, etc.).

Let us consider the stations for which the values of the overall intensity were underestimated, namely: FKO006, IWTH02 and NIG021. Description of local geology for the stations is given in Table 3. The information has been collected from K-NET and KiK-net websites. As can be seen from Table 2 and Fig. 8, the cases of underestimation for both stations FKO002 and IWTH02 correspond to high-amplitude ground motion (large values of overall JMA). Thus, bearing in mind the geotechnical characteristics of soil below station FKO006 (very soft sandy soil) and below station IWTH02 (soft clayey soil), it is possible to suggest that the peculiarities of soil behavior during large-amplitude ground motion (non-linear phenomena?) are responsible for the small $\mathrm{JMA_{P2}}$–large $\mathrm{JMA_O}$ ratio and correspondent underestimation of the overall intensity for these cases. At the same time, we should note that peculiarities of source process may also bring an important contribution to uncertainty of the prediction. The

Table 4 Standard errors of regression calculated for various types of regression and various time intervals from the P-wave arrival

Regression	P-wave window, sec						
	2.0	3.0	4.0	5.0	6.0	7.0	8.0
	Threshold level TL, JMA_I (see text)						
	0.5	0.75	1.0	1.25	1.50	1.75	2.0
Linear							
$JMA_O = a + bJMA_P$	0.67	0.60	0.55	0.52	0.49	0.47	0.46
Multiple							
$JMA_O = a + bJMA_P + cM_W$	0.56	0.53	0.49	0.47	0.45	0.44	0.43
Multiple							
$JMA_O = a + bJMA_P + cM_W + dR$	0.51	0.50	0.47	0.46	0.45	0.44	0.43
Multiple							
$JMA_O = a + bJMA_P + c\log_{10}(\tau_C)$	0.60	0.56	0.52	0.50	0.48	0.47	0.46

considered earthquake of March 20, 2005, was characterized by a small rupture 3 s before the main rupture (Horikawa 2006).

Station NIG021 reveals two cases of extreme underestimation for two large-magnitude earthquakes occurred approximately in the same location in the same day (Table 2). The records were obtained at relatively small epicentral distances (20–30 km, Fig. 8). Most likely the peculiarities of earthquake source (e.g. directivity effect), rather than soil amplification, are responsible for the small JMA_{P2}–large JMA_O ratio. However, it seems that the calculated values of overall intensity, in their turn, are overestimated for these records.

4 Discussion

Table 4 summarizes the values of the standard error of regression σ obtained for various variants of the regression and various time intervals from the P-wave arrival (the P-wave window). In general, the regression error becomes smaller when considering, besides the preliminary intensity, the additional parameters e. g. earthquake magnitude, hypocentral distance R, and characteristic period. The regression error also decreases with the increase of duration of the P-wave window used for estimations of the preliminary intensity.

The uncertainty in estimation of the overall intensity may be represented by the aleatory and the epistemic components. The aleatory uncertainty is caused by inherent random variability of the ground motion parameters. The epistemic uncertainty reflects the incomplete knowledge of the nature of seismic motion and limitations of the technique applied for an analysis. In other words, the aleatory uncertainty describes the disagreement between observations and predictive models, which is due to the absence of a physical explanation or due to the variables that are not included in the predictive equations. Thus, the aleatory component of uncertainty, in principle, may be transformed into epistemic component by identifying and quantifying the additional critical parameters of the model (e.g. Bommer et al. 2004).

As can be seen, the variability in scaling relation between the overall intensity and the preliminary intensity has been reduced after introducing additional parameters (magnitude and distance) into the regression equations, even there is the inherent uncertainty in these additional variables. Another critical parameters in the EEW are the characteristics of earthquake source related to the complex processes of nucleation and growth of an earthquake. The scatter caused by the randomness of the source-rupture processes may be reduced by the increase of the length of the time window from the P-wave arrival used for determination of the preliminary intensity. The increase of the time interval also allows eliminating the influence of mistaken determination of the moment of P-wave arrival. It seems that time interval of 4–5 s from the P-wave arrival may be considered as sufficient for reliable estimations of the overall intensity (see also Yamamoto et al. 2008).

Analysis of the datasets, which contain the data from only shallow and only deep earthquakes, as well as the datasets, which contain the data obtained separately by the K-NET and KiK-net networks, did not show a prominent difference between the standard errors of the $\mathrm{JMA_O}$–$\mathrm{JMA_P}$ relationships. However, in this study we consider the generalized dataset combining data from all regions of Japan. The subduction zone earthquakes occurring in the Pacific plate in NE Japan may produce anomalously large ground accelerations with high-frequency signals (Furumura and Kennett 2005). Thus, it seems that the region-dependent subsets of the data should be also analyzed.

When considering the specific stations, the site-specific behavior of the relationships can be revealed. Figure 9 shows, as the examples, distribution of the $\mathrm{JMA_O}$–$\mathrm{JMA_P}$ pairs for three stations—IWT007, NIG021 and NIGH12. We selected these stations because they accumulated several records in a wide range of $\mathrm{JMA_O}$ values and they are characterized by different geotechnical properties of the soil. The site conditions for the stations are as follows. Station IWT007: gravelly soil ($V_S < 400$ m/s, $V_P > 2{,}200$ m/s) up do depth of 20 m. Stations NIG021: a thin (5–7 m) layer of gravelly soil ($V_S < 400$ m/s, $V_P < 1{,}500$ m/s) over soft rock ($V_S > 500$ m/s, $V_P < 2{,}100$ m/s). Station NIGH12: gravelly soil ($V_S < 500$ m/s, $V_P < 1{,}000$ m/s), thickness about 10–15 m; sandy soil (V_S 700–750 m/s, V_P 2,000 m/s), thickness about 30 m; weathered granite and tuff (V_S 800 m/s, V_P 2,300 m/s). Two stations located on gravelly soil with relatively large V_P/V_S ratios (IWT007 and NIG021) show, in general, the "small $\mathrm{JMA_P}$–large $\mathrm{JMA_O}$" behavior of the relationship. The station NIGH12 located on gravelly and sandy soils with a smaller V_P/V_S ratios and a smooth velocity change between the layers reveals the smaller JMAo values than the other two considered stations for the same JMAp estimations.

It seems that the influence of local geology, may significantly contribute to the uncertainty in the $\mathrm{JMA_P}$–$\mathrm{JMA_O}$ scaling relation. Thus the soil-specific, or even the station-specific, models should be developed to reduce the uncertainty in prediction of damage potential in the EEW systems. If the number of records at a station is not sufficient for development of the station-dependent scaling relation, the station-dependent coefficient ΔJMA_{ST} may be used for adjustment of generalized model as

$$\begin{gathered}\mathrm{JMA_{OP}} = a + b\mathrm{JMA_P} + \Delta\mathrm{JMA_{ST}} \\ \Delta\mathrm{JMA_{ST}} = \left(\sum_{i=1}^{n}\mathrm{JMA_{OO}} - F(\mathrm{JMA_P})\right)/n \end{gathered} \tag{6}$$

where $\mathrm{JMA_{OP}}$ is the predicted overall intensity; $\mathrm{JMA_{OO}}$ is the observed overall intensity;$\Delta\mathrm{JMA_{ST}}$ is the empirically derived station-dependent coefficient evaluated by averaging of residuals between the values of the observed overall intensity and the values predicted using the generalized model $F(\mathrm{JMA_P})$. The coefficients evaluated for the considered stations (Fig. 9) are listed in Table 5. As can be seen, the generalized model significantly overestimate intensity for station NIGH12.

Table 5 Station-dependent coefficients for adjustment of the predictions based on the generalized scaling models

Station	Time interval from the P-wave arrival			
	Predictions based on M_W		Predictions based on τ_C	
	2 s	6 s	2 s	6 s
IWT007	−0.62	0.32	0.38	0.26
NIG021	−0.18	0.36	0.51	0.16
NIGH12	−1.05	−0.61	−0.23	−0.89

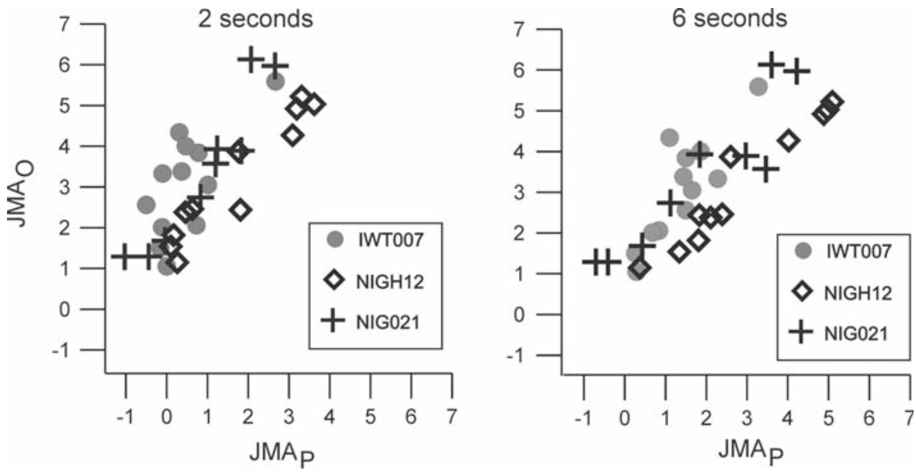

Fig. 9 Distribution of the JMA instrumental intensity calculated for the entire earthquake records (JMA_O) versus the intensity estimated for the initial portions of ground motion (JMA_P) for particular stations

5 Conclusion

We investigated the scaling relationship between the JMA instrumental intensity measured using (a) the whole earthquake recordings (JMA_O, overall intensity) and (b) the particular time intervals of various durations (2.0,…, 8.0 s) starting from the P-wave arrival (JMA_P, preliminary intensity). The performance of the relationship in respect of its utilization in the EEW issues has been studied. The dataset included 3,660 records from 55 events with magnitude range M_W 4.1–7.4 occurred in 1999–2008 in Japan. The earthquakes were recorded by the K-NET and the KiK-net nation-wide networks. The relationships, in contrast with the recent results obtained by Yamamoto et al. (2008), do not require knowledge on regional path-attenuation (Q-model) and they may be used ether without or together the additional information on the earthquake magnitude and distance. The performance of the relationship in respect of its utilization in the Earthquake Early Warning issues has been studied.

The quality of predictions of macroseismic intensity (JMA scale) of the strongest part of shaking from the initial portion of earthquake ground motion depends on (a) duration of the portion and (b) availability of additional information about the earthquake characteristics (magnitude and distance). The time interval of 4–5 s from the P-wave arrival may be considered as sufficient, at least for magnitudes $M < 7.5$, for reliable estimations of the

Table 6 Parameters of the relation between the overall intensity (JMA_O) and the preliminary intensity (JMA_P)

Regression	Coefficients			St. error
	a	b	c	σ
2 s				
$JMA_O = a + bJMA_P$	2.375	0.791	–	0.67
$JMA_O = a + bJMA_P + cM_W$	−1.213	0.706	0.595	0.56
$JMA_O = a + bJMA_P + c\log_{10}(\tau_C)$	2.224	0.793	0.932	0.60
3 s				
$JMA_O = a + bJMA_P$	2.179	0.824	–	0.60
$JMA_O = a + bJMA_P + cM_W$	−0.838	0.744	0.500	0.53
$JMA_O = a + bJMA_P + c\log_{10}(\tau_C)$	2.052	0.824	0.794	0.56
4 s				
$JMA_O = a + bJMA_P$	2.026	0.815	–	0.55
$JMA_O = a + bJMA_P + cM_W$	−0.693	0.750	0.448	0.49
$JMA_O = a + bJMA_P + c\log_{10}(\tau_C)$	1.922	0.814	0.665	0.52
5 s				
$JMA_O = a + bJMA_P$	1.872	0.838	–	0.52
$JMA_O = a + bJMA_P + cM_W$	−0.579	0.776	0.404	0.47
$JMA_O = a + bJMA_P + c\log_{10}(\tau_C)$	1.784	0.839	0.486	0.50
6 s				
$JMA_O = a + bJMA_P$	1.814	0.829	–	0.49
$JMA_O = a + bJMA_P + cM_W$	−0.795	0.781	0.422	0.45
$JMA_O = a + bJMA_P + c\log_{10}(\tau_C)$	1.738	0.830	0.404	0.48
7 s				
$JMA_O = a + bJMA_P$	1.717	0.846	–	0.47
$JMA_O = a + bJMA_P + cM_W$	−0.755	0.797	0.400	0.44
$JMA_O = a + bJMA_P + c\log_{10}(\tau_C)$	1.676	0.840	0.282	0.46
8 s				
$JMA_O = a + bJMA_P$	1.694	0.834	–	0.46
$JMA_O = a + bJMA_P + cM_W$	−1.055	0.800	0.434	0.43
$JMA_O = a + bJMA_P + c\log_{10}(\tau_C)$	1.649	0.832	0.236	0.46

overall intensity with average standard error of about 0.5 units of JMA. The uncertainty in the prediction of macroseismic intensity may be also reduced when considering generalized local site conditions in the scaling relations or creating the station-specific models. At present we suggest to use in the real-time EEW systems the generalized (site-independent) scaling relations, the parameters of which are given in Table 6, together with the empirically-derived station-dependent coefficients, examples of which are shown in Table 5.

Among the future tasks for optimitization of the proposed scaling relation that can be used for rapid estimation of damage potential in the EEW system, we can mention the following. The database, which is used for analysis of scaling relations, should be expanded by consideration of suitable strong motion records obtained by seismic networks worldwide (e.g. Taiwan, California, Italy, Greece, New Zealand). This would allow comprehensive analysis of influence of local (soil conditions) and regional (propagation path) geological conditions on the scaling relations. For example, the most of the K-NET and KiK-net stations in the northeastern Japan, the data from which are used in this study, is installed on rocky sites covered by very thin superficial layers. In contrast, the majority of strong-motion stations in Taiwan (TSMIP network) is installed on deep plain (Western plain) and alluvium basins (Taipei and Ilan basins).

We selected the JMA intensity in our study because seismic intensity scales are still widely used for simple and fast estimation of damage levels and the EEW issues are based on the JMA intensity assessments. However, it has been shown (e.g. Nakamura et al. 2006) that JMA intensity may not have a strong correlation with building damage. The sophisticated destructive power indices (e.g. elastic response velocity) should be used for robust prediction of damage level and, therefore, should be also adopted in the EEW systems.

Acknowledgments This research was funded by the SAFER project (http://www.saferproject.net/) of the EU's Sixth Framework Programme, contract No. 036935. Support from the Japan Society for Promotion of Science (JSPS) is very much appreciated. The authors are very grateful to two anonymous reviewers for valuable comments and suggestions that allow improving the manuscript. The authors would also like to thank the National Research Institute for Earth Science and Disaster Prevention, Japan for providing K-NET and KiK-net data.

References

Allen RM (2004) Rapid magnitude determination for earthquake early warning. In: Manfredi G et al (ed) The many facets of seismic risk (Proceedings of the "Workshop on multidisciplinary approach to seismic risk problems"). Universita degli Studi di Napoli, Napoli, pp 15–24

Allen RM (2007) The ElarmS earthquake early warning methodology and application across California. In: Gasparini P et al (ed) Earthquake early warning systems. Springer, Berlin, pp 21–43. doi:10.1007/978-3-540-72241-0

Allen RM, Gasparini P, Kamigaichi O, Boese M (2009) The status of earthquake early warning around the world: an introductory overview. Seism Res Lett 80(5):682–693. doi:10.1785/gssrl.80.5.682

Aoi A, Obara S, Hori S, Kasahara K, Okada Y (2000) New strong observation network KiK-net. EOS Trans Am Geophys Union 81, F863

Aoi S, Kunugi T, Adachi S, Nakamura H, Morikawa N, Abara K, Fujiwara H (2008) Implementation of real-time capability of strong-motion seismographs network KiK-net. In: Programme and abstracts, the 7th general assembly of Asian seismological commission and the 2008 Fall meeting of seismological society of Japan, 24–27 November 2008, Tsukuba, Japan, p 26

Bommer JJ, Scherbaum F, Cotton F, Bungum H, Sabetta F (2004) Discussion "Uncertainty analysis of strong-motion and seismic hazard" by R. Sigbjornsson and N. N. Ambraseys. Bull Earthquake Eng 2, pp 261–267

Doi K, Tsukada S, Aketagawa T, Kiyomoto M, Matsumori N, Kamigaichi O (2008) Earthquake early warning in Japan—Provision to general public and its results. In: Programme and abstracts, the 7th general assembly of Asian seismological commission and the 2008 fall meeting of seismological society of Japan, 24–27 November 2008, Tsukuba, Japan, p 23

Furumura T, Kennett BLN (2005) Subduction zone guided waves and the heterogeneity structure of the subducted plate: intensity anomalies in northern Japan. J Geoph Res 110:B10302.1-B10302.27 doi:10.1029/2004JB003486

Horikawa H (2006) Rupture process of the 2005 west off fukuoka prefecture, Japan, earthquake. Earth Planets Space 58(1):87–92

Hoshiba M, Kamigachi O, Saito M, Tsukada S, Hamada N (2008) Earthquake early warning starts nationwide in Japan. EOS Trans Am Geophys Union 89(8):73–80

Kamigaichi O, Saito M, Doi K, Matwumori T, Tsukada S, Takeda K, Shimoyama T, Nakamura K, Kiyomoto M, Watanabe Y (2009) Earthquake early warning in Japan: warning the general public and future prospects. Seism Res Lett 80(5):717–726. doi:10.1785/gssrl.80.5.717

Kanamori H (2005) Real-time seismology and earthquake damage mitigation. Ann Rev Earth Planet Sci 33:195–214

Kanda K, Nasu T, Miyamura M (2008) Site-specific earthquake early warning system for hazard mitigation. In: Programme and abstracts, the 7th general assembly of Asian seismological commission and the 2008 fall meeting of seismological society of Japan, 24–27 Nov 2008, Tsukuba, Japan, p 25

Kinoshita S (1998) Kyoshin Net (K-NET). Seism Res Lett 69:309–332

Kunugi T, Aoi S, Nakamura N, Fujiwara H, Morikawa N (2008) A real-time processing of seismic intensity. Zisin 2:243–252 (in Japanese)

Nakamura Y, Sakai Y, Kato D (2006). Investigation of destructive power indices of strong motion using building damage data and strong motions recorded in the 2004 Niigata-Chuetsu, Japan, earthquake. http://yukiko.eng.niigata-u.ac.jp/papers/2006ncee.pdf

Nakamura Y, Saita J (2007) UeEDAS, the earthquake warning system: today and tomorrow In: Gasparini P et al (ed) Earthquake early warning systems. Springer, Berlin, pp 249–280. doi:10.1007/978-3-540-72241-0

Shabestari KhT, Yamazaki F (2001) A proposal of instrumental seismic intensity scale compatible with MMI evaluated from three-component acceleration records. Earthq Spectra 17(4):711–723

Sokolov V, Furumura T (2008) Comparative analysis of two methods for instrumental intensity estimations using the database accumulated during recent large earthquakes in Japan. Earthq Spectra 24(2): 513–532. doi:10.1193/1.2923918

Sokolov V, Wenzel F, Furumura T (2009) On estimation of earthquake magnitude in earthquake early warning systems. Earth, Planets, Space 61(12):1275–1285

Ueda T, Kurahashi S, Masaki K, Irikura K (2008) Improvement of earthquake early warning intensity estimation from P-wave's amplitudes, In: Programme and abstracts, the 7th general assembly of Asian seismological commission and the 2008 fall meeting of seismological society of Japan, 24–27 November 2008, Tsukuba, Japan, p 28

Wu YM, Kanamori H (2005) Rapid assessment of damage potential of earthquake in Taiwan from the beginning of P waves. Bull Seism Soc Am 95:1181–1185

Wu YM, Kanamori H, Allen RM, Hauksson E (2007) Determination of earthquake early warning parameters, τ_C and P_d for southern California. Geophys J Int 170:711–717

Yamamoto S, Rydelek P, Horiuchi S, Wu C, Nakamura H (2008) On the estimation of seismic intensity in earthquake early warning systems. Geophys Res Lett 35:L07302. doi:10.1029/2007/GL033034